Solid State Ionics 61 (1993) 83–91
North-Holland

Synthesis of strontium and barium cerate and their reaction with carbon dioxide

M.J. Scholten [1], J. Schoonman
Laboratory for Applied Inorganic Chemistry, Delft University of Technology, Julianalaan 136, 2628 BL Delft, The Netherlands

and

J.C. van Miltenburg, H.A.J. Oonk
Department for Interfaces and Thermodynamics, Utrecht University, Padualaan 8, 3584 CH Utrecht, The Netherlands

The log p_{CO_2} versus $1/T$ relationships of the equilibria (1) $ACO_3 + CeO_2 \rightleftarrows ACeO_3 + CO_2$ and (2) $ACO_3 \rightleftarrows AO + CO_2$, in which A = Sr or Ba, were investigated. The methods which have been used are: thermodynamic equilibrium calculations, simultaneous thermogravimetry–differential thermal analysis and high-temperature X-ray diffraction. In pure N_2 atmosphere, the synthesis of the cerates proceeds via (1) $ACO_3 \rightarrow AO + CO_2$ and (2) $AO + CeO_2 \rightarrow ACeO_3$, which is not calculated thermodynamically, but is apparently kinetically more favourable at low temperatures. $SrCeO_3$ and $BaCeO_3$ react with 1 atm CO_2 below 1190°C and 1185°C, respectively. For mixtures of CO_2 with other gases, the decomposition temperatures can be estimated from the figures presented.

1. Introduction

Solid solutions based on the perovskite type oxides strontium and barium cerate have been explored for their use in solid oxide fuel cells and hydrogen sensors [1].

A major disadvantage of the cerates is their instability in CO_2 containing atmospheres as pointed out by Uchida et al. [2]. They showed that $SrCe_{0.95}Yb_{0.05}O_{3-\alpha}$ reacts below about 800°C with an atmosphere containing 10% CO_2. Furthermore, it has been demonstrated by Luyten et al. [3] that strontium cerate is not stable in a simulated coal gasification atmosphere containing 0.0033 vol% H_2S at 800°C, since SrS and CeO_2 are formed. Yajima et al. [4] have recently investigated $CaZrO_3$ because zirconates are less reactive with CO_2.

The synthesis of $SrCeO_3$ has been studied before experimentally by Keler et al. [5] and Zheng et al. [6].

We have investigated the following equilibria:

$$SrCO_3 + CeO_2 \rightleftarrows SrCeO_3 + CO_2, \quad (1)$$

$$SrCO_3 \rightleftarrows SrO + CO_2, \quad (2)$$

$$BaCO_3 + CeO_2 \rightleftarrows BaCeO_3 + CO_2, \quad (3)$$

$$BaCO_3 \rightleftarrows BaO + CO_2, \quad (4)$$

by using simultaneous thermogravimetry–differential thermal analysis (TG–DTA), in a pure 1 atm CO_2 or N_2 flow, up to 1500°C, and high-temperature X-ray diffraction (HT–XRD), in pure 1 atm N_2 flow, up to 900°C. The experimental results are compared with thermodynamic equilibrium calculations.

2. Experimental aspects

2.1. Samples

$SrCO_3$ (Merck 7861), $BaCO_3$ (Merck 1714: >99%), CeO_2 (Fluka 22390: >99%) were used. The 50 mol% $SrCO_3$ or $BaCO_3$–50 mol% CeO_2 mixtures were made by dry mixing of the powders in an agate mortar.

[1] Author to whom correspondence should be addressed.

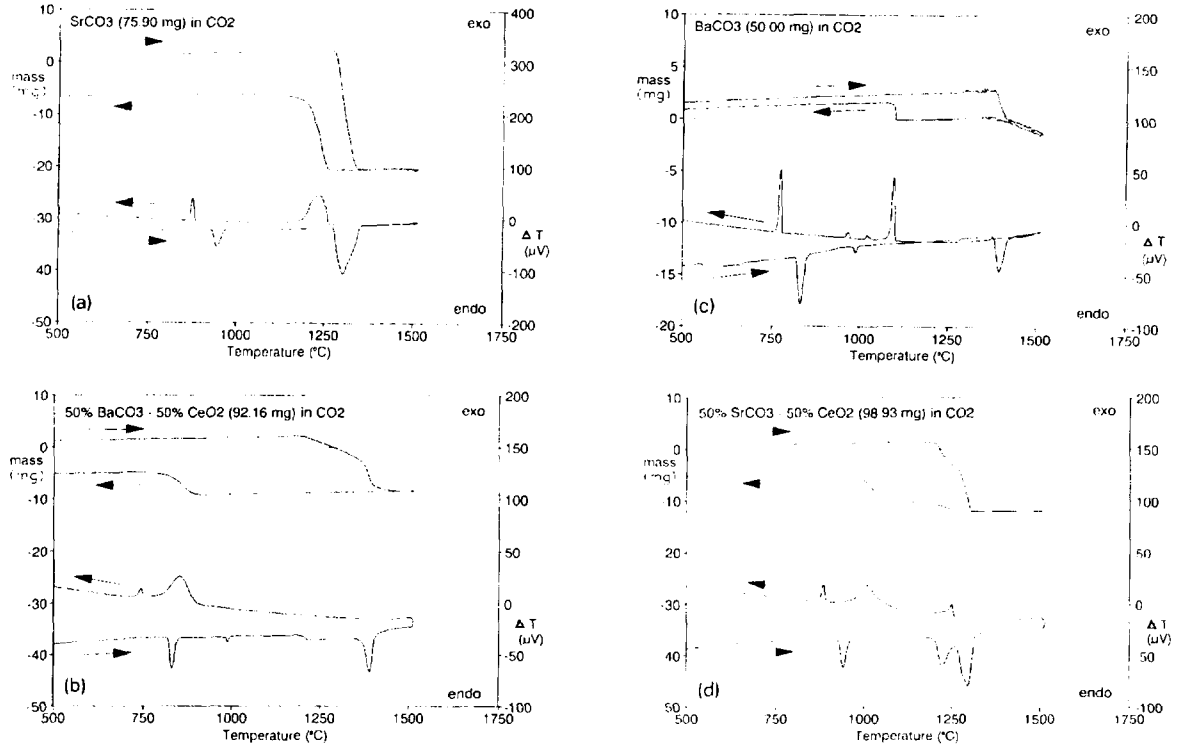

Fig. 1. TG–DTA curves in CO_2. The TG and ΔT data are presented in the upper and lower part of the figure, respectively.

2.2. TG–DTA

A Setaram TG–DTA 92 was used for simultaneous thermogravimetry and differential thermal analysis (TG–DTA) from ambient temperature up to 1500°C. A Pt-crucible was used, although it reacts with the $BaCO_3$ melt. The heating rate was 20°C/min. A flow of CO_2 or N_2 was passed over the sample. Pt–Pt/10%Rh thermocouples were used. In table 1 a comparison is made between the present and Iwafuchi's [7] and Erné's [8] determination of phase transition onset temperatures in $SrCO_3$ and $BaCO_3$. The agreement is good.

2.3. HT-XRD

For the high-temperature X-ray diffraction (HT-XRD) study an Enraf Nonius Guinier–Lenné camera was employed using Cu Kα radiation. The powder samples, present on a Pt-grid, were heated with

Table 1
DTA onset temperatures of transitions in $SrCO_3$ and $BaCO_3$.

Sample	Atmosphere	Temperature (°C)		Ref.
		orthorhombic–rhombohedral	rhombohedral–cubic	
$SrCO_3$	CO_2	923	–	
	N_2	926	–	[7]
$SrCO_3$	CO_2	932	–	
	N_2	not determined	–	[8]
$SrCO_3$	CO_2	928	–	
	N_2	929	–	this study
$BaCO_3$	CO_2	815	not determined	
	N_2	808	not determined	[7]
$BaCO_3$	CO_2	810	977	
	N_2	not determined	not determined	[8]
$BaCO_3$	CO_2	817	980	
	N_2	807	971	this study

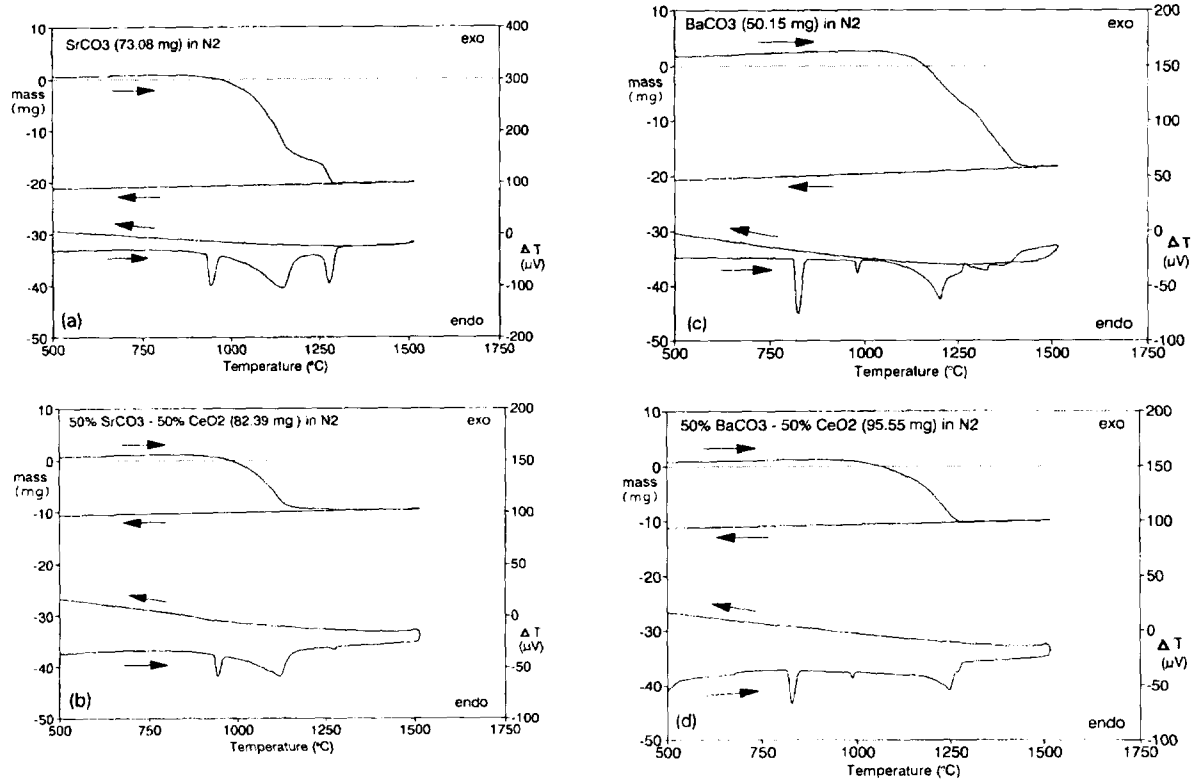

Fig. 2. TG–DTA curves in N_2. The TG and ΔT data are presented in the upper and lower part of the figure, respectively.

a rate of 600°C/h from ambient temperature up to 700°C, and with a rate of 10°C/h between 700 and 900°C in a N_2 flow. The temperature was measured with a Pt–Pt/10% Rh thermocouple.

3. Results and discussion

3.1. Thermodynamic calculations

The thermodynamic data which were used were taken from Sorokina et al. [9] for $SrCeO_3$, from Levitskii et al. [10] for $BaCeO_3$, and from Barin [11] for all the other compounds. The calculated log p_{CO_2}–$1/T$ relationships of the equilibria (1), (2), (3) and (4) are presented in figs. 5 and 6 by solid lines. The change in Gibbs free energy of the reaction $AO+CeO_2 \rightarrow ACeO_3$ is always negative under the conditions presented in figs. 5 and 6, which means that $ACeO_3$ does not decompose into AO plus CeO_2.

Table 2
TG weight loss in N_2.

Sample (mol%)	Theoretical weight loss (%)	Measured weight loss (%)	Fractional extent of reaction
$SrCO_3$	29.81	29.83	100.06
50% $SrCO_3$, 50% CeO_2	13.76	13.89	100.92
$BaCO_3$	22.30	22.52	100.98
50% $BaCO_3$, 50% CeO_2	11.91	12.04	101.08

3.2. Experiments

The TG–DTA curves are presented in fig. 1 (CO_2-flow) and fig. 2 (N_2-flow). In table 2 the TG weight loss data in N_2 atmosphere are given. They are determined by taking the difference in wt% at 500°C between the heating and cooling cycle. The experimental weight loss is 100.01–101.08% of the value expected for complete decomposition, which means

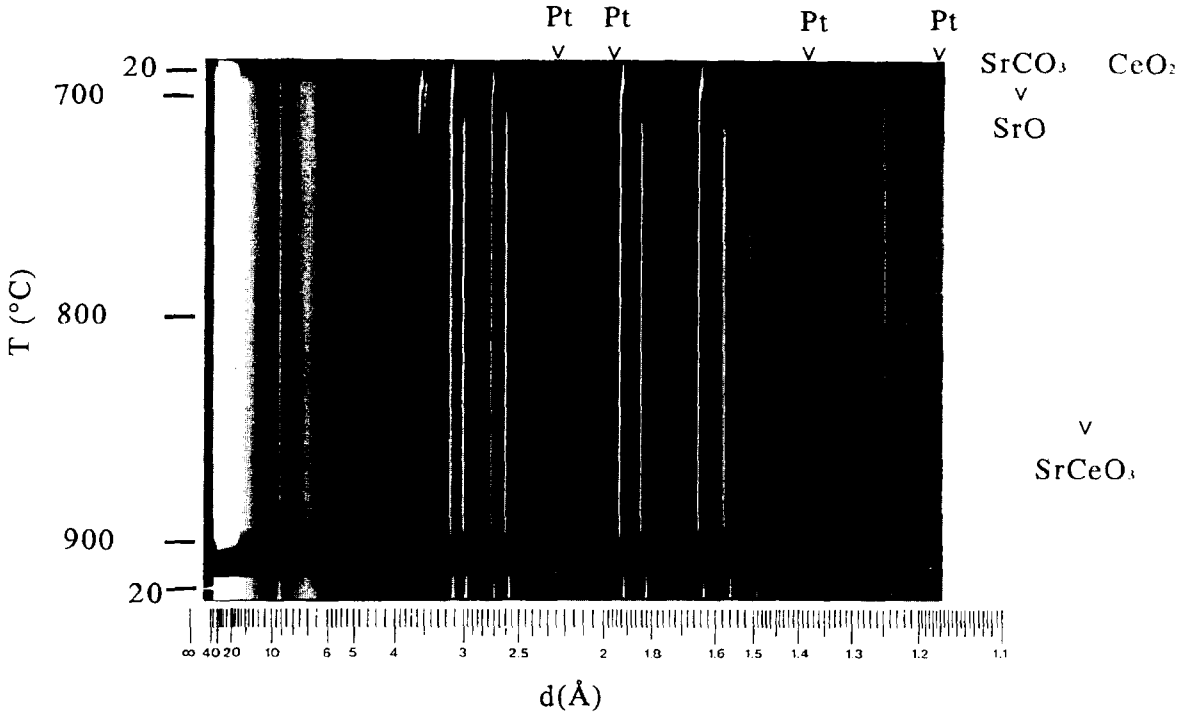

Fig. 3. HT-XRD of 50% $SrCO_3$–50% CeO_2 in N_2.

Table 3
TG onset temperatures of decomposition of carbonates or synthesis of cerates.

Sample (mol%)	Atm. (1 atm)	Temp. (°C)
$SrCO_3$	CO_2	1275
	N_2	845
50% $SrCO_3$, 50% CeO_2	CO_2	1190
	N_2	800
$BaCO_3$	CO_2	1376 (DTA)
	N_2	930
50% $BaCO_3$, 50% CeO_2	CO_2	1185
	N_2	850

that the loss of carbon dioxide is complete.

From the TG–DTA curves the TG onset temperatures of the decomposition of carbonate or synthesis of cerate are determined and these temperatures are presented in table 3 and plotted in figs. 5 and 6.

3.2.1. $SrCO_3$

The decomposition of $SrCO_3$ at different CO_2 pressures has been measured before by Lander [12] and Baker [13].

In our TG–DTA experiments $SrCO_3$ starts to decompose to SrO at 1275°C in pure CO_2 at atmospheric pressure, which is slightly higher than the 1259°C found by Baker [13]. These measured temperatures of decomposition are much higher than the calculated ones. Two explanations for this discrepancy may be given: (1) the experimental decomposition curve is a non-equilibrium curve or (2) the thermodynamic data available are not correct.

Because of the fact that in pure CO_2 the changes in the TG–DTA signals are sharp and that decomposition takes place at almost the same temperature as the reverse reaction of SrO to $SrCO_3$, it is believed that the experimental point at 1 atm is at equilibrium, which implies that the thermodynamic data are not correct. The thermodynamic properties of $SrCO_3$ should be reinvestigated, which was also con-

cluded by Busenberg et al. [14]. We are now evaluating the thermodynamic properties of $SrCO_3$ and remeasuring the low temperature heat capacities by adiabatic calorimetry. The results of this study will be published elsewhere.

In N_2-flow, the HT-XRD data show the direct complete decomposition of $SrCO_3$ to SrO. The TG-DTA curve shows, however, two decomposition peaks. Since the second step in TG-DTA starts at a temperature which is almost equal to the decomposition temperature in pure CO_2, this "two step" decomposition is probably due to the fact that the partial pressure of CO_2 increases during decomposition. The changes of the TG-DTA signals are gradual, indicating that kinetics play an important role.

3.2.2. $BaCO_3$

The decomposition of $BaCO_3$ at different CO_2 pressures has been measured before by Lander [12] and Baker [15].

In our TG-DTA experiments the $BaCO_3$ starts to melt and loose carbon dioxide at 1380°C in pure CO_2 at atmospheric pressure. This is in good agreement with the data of Baker [15]. The melt attacks the Pt-crucible.

The measured temperatures of decomposition to BaO of Lander [13] at low pressures of CO_2 are in good agreement with the calculated ones.

In N_2 atmosphere the decomposition of $BaCO_3$ starts with the reaction to BaO, but after the CO_2 pressure has increased too much the decomposition proceeds to produce a melt which attacks the Pt-crucible, resulting in a very irregular DTA curve. The HT-XRD data demonstrate that $BaCO_3$ decomposes in N_2 to form solid BaO. The rhombohedral $BaCO_3$ which exists between 807°C and 971°C is not described in the JCPDS file.

3.2.3. 50% $SrCO_3$–50% CeO_2 mixture

In pure CO_2 at atmospheric pressure the reaction proceeds as follows. First the reaction $SrCO_3+CeO_2 \rightarrow SrCeO_3+CO_2$ takes place, starting at 1190°C, which is significantly higher than the calculated temperature (see fig. 5). This discrepancy

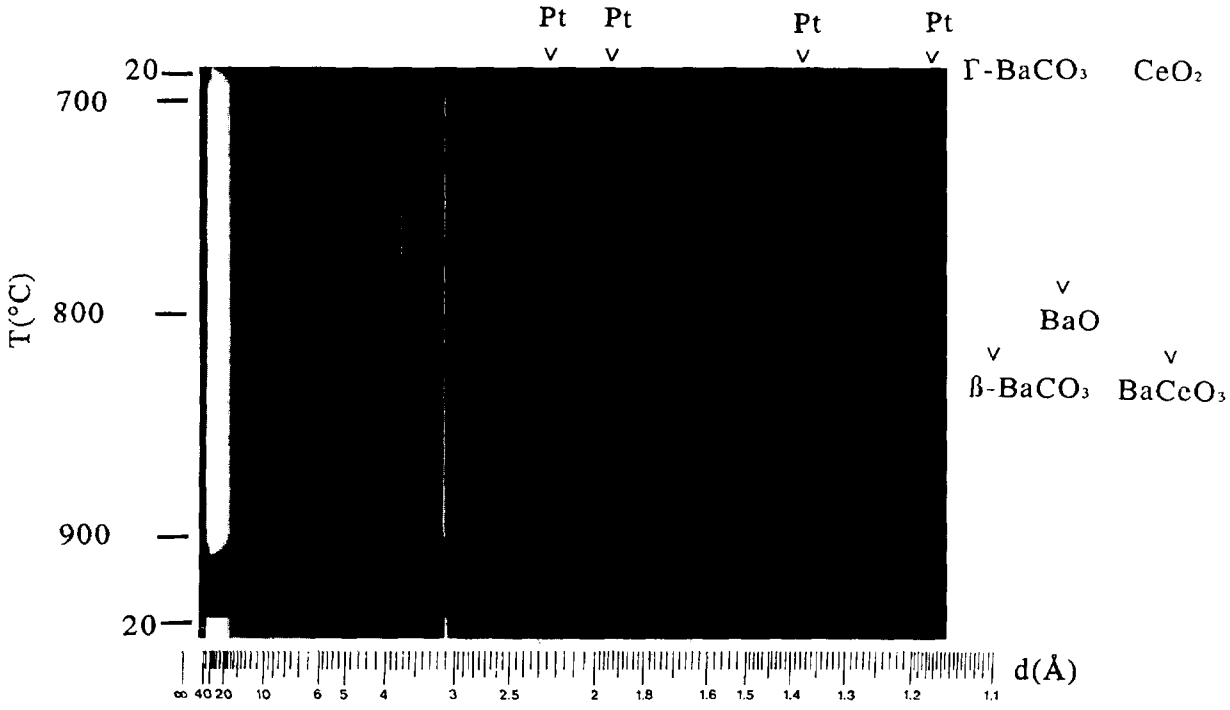

Fig. 4. HT-XRD of 50% $BaCO_3$–50% CeO_2 in N_2.

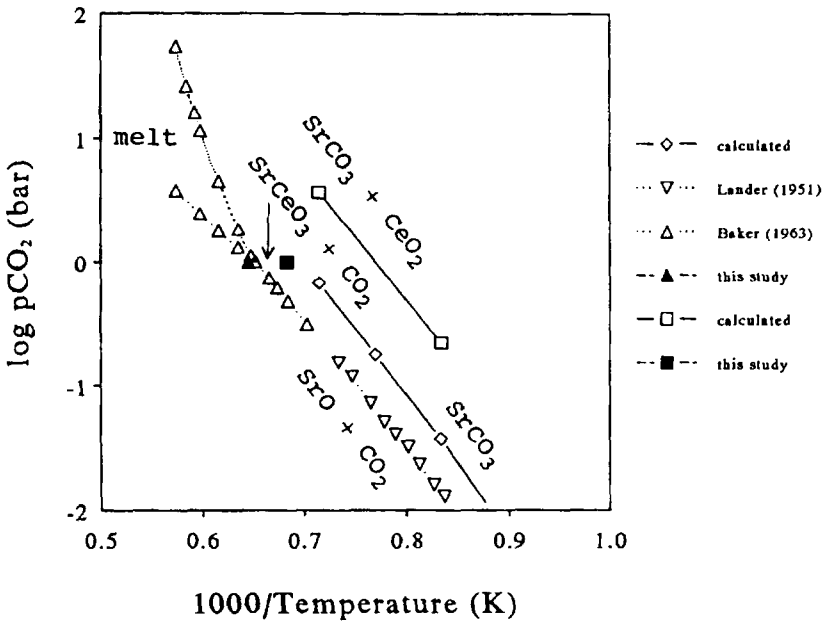

Fig. 5. Stability of SrO and $SrCeO_3$ in CO_2 containing atmosphere.

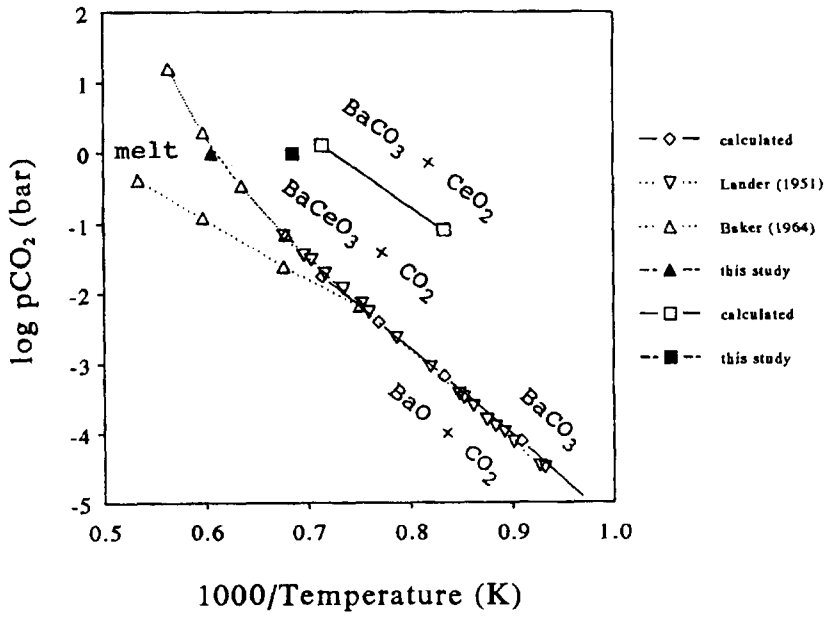

Fig. 6. Stability of BaO and $BaCeO_3$ in CO_2 containing atmosphere.

Table 4
The calcining of strontium and barium cerates.

Dopant	Starting materials			Calcining				Ref.
	Ca Sr Ba	Ce	dopant except Ca	crucible	atm.	time (h)	temp. (°C)	
Strontium cerates								
none	c [a]	o [b]	-			4	1400	16
Yb etc.	c	o	o/c		air	5–10	1300–1450	17
Yb	c	o	o		air	10	1350	18
Yb	n [c]	n	n		vacuum		200	19
					air	5	800	
Yb	c	o	o	Al_2O_3		48	1000	20
Y + (Nb or Zr)	c	o	o				1400	4
Yb	c	o	o		air	10	1400	3
Yb	o	o	o	Pt in Al_2O_3	air	6	1450	21
Barium cerates								
Bi						10–12	1000–1200	22
none	c	o	-			4	1400	16
none	c	o	-	Pt		4	1250	23
Y	c	o	o	Pt		4	1100	23
Ho, Nd, La	c	o	o	Pt		4	1100	24
Nd, La, Y, Ca	c	o	o		air	5	1250	25
Yb	c	o	o	Al_2O_3		48	1000	20
Gd	c	o	o		air		1100	26
					air	10	1400	
Ca,Eu,Gd,Nd, Yb	c	o	o	Al_2O_3		5	1250	27
Yb,Y,Gd,La	c	o	o			6	1000	28
Gd,La,Nd,Y,Yb	c	o	o	Al_2O_3	air	15	1250	29

[a] c: carbonate; [b] o: oxide; [c] n: nitrate.

may be caused by incorrect thermodynamic data (see also $SrCO_3$!). This reaction is not completed at around 1275 °C, so now the decomposition of $SrCO_3$ takes place. From the "two step" reverse reaction during cooling in CO_2, one can conclude that the reaction to $SrCeO_3$ did not go to completion during heating.

In pure N_2 at atmospheric pressure the HT-XRD data (fig. 3) reveal that the reaction proceeds as follows:

$SrCO_3 \rightarrow SrO + CO_2$,

$SrO + CeO_2 \rightarrow SrCeO_3$,

which is not calculated thermodynamically, but is apparently kinetically more favourable at low temperatures. Zheng et al. [6] have investigated the synthesis of $SrCeO_3$ by DTA, TG and XRD and stated that the reaction proceeds in three steps: (1) $SrCO_3$ decomposition at 925 °C (endothermic), (2) $SrCeO_3$ formation (endothermic) and (3) sintering (endothermic).

Their observations should be explained as follows. Their first endothermic peak is the phase transition in $SrCO_3$ at around 925 °C. Their second step is the decomposition of $SrCO_3$ and subsequent formation of $SrCeO_3$. Their last step is the same as the second step only at an increased CO_2 partial pressure and, therefore, increased temperature.

3.2.4. 50% $BaCO_3$–50% CeO_2 mixture

In pure CO_2 at atmospheric pressure the reaction of $BaCO_3 + CeO_2 \rightarrow BaCeO_3 + CO_2$ starts at 1155 °C, which is slightly higher than the calculated temper-

Table 5
The sintering of strontium and barium cerates.

Preconsolidation		Sintering				Ref.
binder	pressure (MPa)	atm.	time (h)	temp. (°C)	rel. density (%)	
Strontium cerates						
						[16]
		air	5–10	1350–1450		[17]
			10	1440	96	[18]
ethylene glycol	390	air	10	1400	84	[19]
					open por. < 1%	
	280	air	96	1350	75–85	[20]
		air	10	1460		[4]
		air	10	1500	82–88	[3]
					open por. 18–12%	
poly vinyl alcohol	200	air	12 (150°C/h)	1590	97	[21]
Barium cerates						
	290–490	air	10–12	1200		[22]
						[16]
ethyl cellulose	240	air	4	1350		[23]
	240		4	1350	por. < 6%	[24]
	200	air	10	1500		[25]
	280	air	96	1350	> 75	[20]
	390	N_2/5% H_2	10	1475	> 90	[26]
					open por. < 1%	
		air	12	1500	> 75	[27]
		air	96	1450	> 85	[28]
camphor 1 mass%	490	air	10	1500		[29]

ature (see fig. 6). Subsequently the decomposition of $BaCO_3$ to BaO takes place. A hysteresis exists in the temperatures of thermal and gravimetric effects in the heating and cooling curve. This is probably due to the formation of a melt.

In N_2 at atmospheric pressure the reaction proceeds analogous to the mechanism of the strontium compounds as described in the previous section (see fig. 4).

4. Conclusions

The thermodynamic properties of $SrCO_3$, $SrCeO_3$ and $BaCeO_3$ should be reinvestigated. The results of this evaluation and the measurements will be published elsewhere.

The synthesis of the cerates proceeds in pure N_2 atmosphere via (1) $ACO_3 \rightarrow AO + CO_2$ and (2) $AO + CeO_2 \rightarrow ACeO_3$ (A is Sr or Ba), which is not calculated thermodynamically. Apparently the reaction (1) proceeds kinetically more favourable at low temperatures.

$SrCeO_3$ and $BaCeO_3$ react with pure CO_2 below 1190°C and 1185°C, respectively. For mixtures of CO_2 with other gases, the decomposition temperatures can be estimated from figs. 5 and 6. If one wants to apply these cerates in solid oxide fuel cells or hydrogen sensors, the operating temperatures should be high enough and the partial pressure of CO_2 low enough to avoid the decomposition of the cerate. Further implications of this decomposition will be discussed in the next two sections.

4.1. The sintering of cerates

The decomposition of organic binders at low temperatures will produce carbon dioxide, which will react with the cerate to form carbonate and ceria. The volume of the product is larger than the volume of the starting material (we calculated an increase in volume at room temperature of around 35%). At higher temperatures the carbonate will react back with ceria to cerate, causing a decrease in volume. These changes in volume may be the cause of the low relative density of the sinters! To produce sinters of high relative density one should therefore be able to (1) avoid the use of binders, by using powders of very small grain size or (2) let the binders not decompose to carbon dioxide, by sintering in reducing atmosphere.

In tables 4 and 5 an overview is given of the different procedures used to make sinters of cerates. Only Bonanos et al. [26] have used a reducing atmosphere (N_2/5% H_2) during sintering.

4.2. Pre-treatments in a reducing atmosphere of mixtures of CO and CO_2

Scherban et al. [30] pre-treated the ceramic pellets of cerate at 900°C for 10 h in 1% CO/99% CO_2 and 50% CO/50% CO_2 atmospheres, prior to electrical conductivity measurements below 400°C in air. It is very likely that the formation of $SrCO_3$ and CeO_2 in these CO_2-containing atmospheres has occurred, which may explain the change in color and drop in electrical conductivity.

Acknowledgements

The authors are grateful to Dr. Ir. G. Hakvoort, A. van den Engel and F.E.D. van Halsema for preliminary TGA experiments, to J.F. van Lent and N.M. van der Pers for HT-XRD and to Dr. J.G.M. Becht for comments on the manuscript.

References

[1] H. Iwahara, in: Solid State Ionics, eds. M. Balkanski, T. Takahashi and H.L. Tuller (Elsevier, Amsterdam, 1992) pp. 575–586.
[2] H. Uchida, A. Yasuda and H. Iwahara, Denki Kagaku 57 (1989) 153.
[3] J. Luyten, F. de Schutter, J. Schram and J. Schoonman, Solid State Ionics 46 (1991) 117.
[4] T. Yajima, H. Iwahara, H. Uchida and K. Koide, Solid State Ionics 40/41 (1990) 914.
[5] E.K. Keler and N.A. Godina, J. Inorg. Chem. USSR 2 (1957) 209.
[6] Minhui Zheng, Shuyun Ma and Yanruo Yong, Solid State Ionics-8 Conf. Lake Louise (1991) Abstract S13.
[7] K. Iwafuchi, C. Watanabe and R. Otsuka, Thermochim. Acta 64 (1983) 381.
[8] B.H. Erné, A.J. van der Weijden, A.M. van der Eerden, J.B.H. Jansen, J.C. van Miltenburg and H.A.J. Oonk, CALPHAD 16 (1992) 63.
[9] S.L. Sorokina, Yu.Ya. Skolis, M.L. Kovba and V.A. Levitskii, Russ. J. Phys. Chem. 60 (1986) 186.
[10] V.A. Levitskii, S.L. Sorokina, Yu.Ya. Skolis and M.L. Kovba, Inorg. Mat. 21 (1986) 1190.
[11] I. Barin, Thermochemical Data of Pure Substances (VCH, Weinheim, 1989).
[12] J.J. Lander, J. Am. Chem. Soc. 73 (1951) 5794.
[13] E.H. Baker, J. Chem. Soc. (1963) 339.
[14] E. Busenberg, L.N. Plummer and V.B. Parker, Geochim. Cosmochim. Acta 48 (1984) 2021.
[15] E.H. Baker, J. Chem. Soc. (1964) 699.
[16] V. Longo, F. Ricciardiello and O. Sbaizero, in: Energy and Ceramics, P. Vincenzini, ed. (Elsevier, Amsterdam, 1980) pp. 1123–1130.
[17] H. Iwahara, T. Esaka, H. Uchida and N. Maeda, Solid State Ionics 3/4 (1981) 359.
[18] K. Nagata, M. Nishino and K.S. Goto, J. Electrochem. Soc. 134 (1987) 1850.
[19] N. Bonanos, B. Ellis and M.N. Mahmood, Solid State Ionics 28–30 (1988) 579.
[20] T. Scherban, W.-K. Lee and A.S. Nowick, Solid State Ionics 28–30 (1988) 585.
[21] T. Ohgi, T. Namikawa and Y. Yamazaki, in: Proc. First Intern. Symp. on Ionic and Mixed Conducting Ceramics, eds. T.A. Ramanarayanan and H.L. Tuller (1991) pp. 161–171.
[22] T. Takahashi and H. Iwahara, Energy Conv. 11 (1971) 105.
[23] A.N. Virkar, B.K. Das, S.K. Sundaram and H.S. Maiti, Transact. Indian Ceram. Soc. 41/3 (1982) 63.
[24] M.K. Paria and H.S. Maiti, Solid State Ionics 13 (1984) 285.
[25] H. Iwahara, H. Uchida, K. Ono and K. Ogaki, J. Electrochem. Soc. 135 (1988) 529.
[26] N. Bonanos, B. Ellis, K.S. Knight and M.N. Mahmood, Solid State Ionics 35 (1989) 179.
[27] J.F. Liu and A.S. Nowick, Materials Research Society Symp. Proc. 210, Solid State Ionics II (Boston, USA, 1990) pp. 675–680.
[28] Z.-H. Xu and T.-L. Wen, in: Recent Advances in Fast Ion Conducting Materials and Devices, eds. B.V.R. Chowdari, Q.-G. Liu and L.-G. Chen (World Scientific, Singapore, 1990) pp. 475–479.
[29] R.C.T. Slade and N. Singh, Solid State Ionics 46 (1991) 111.
[30] T. Scherban and A.S. Nowick, Solid State Ionics 35 (1989) 189.